

# Be-implanted GaN: electrical and structural analysis

Y. J. Sun\*, L. S. Tan\*, S. J. Chua\*,<sup>#</sup> and Z. C. Feng<sup>#</sup>

\* Centre for Optoelectronics, Department of Electrical Engineering,  
National University of Singapore, Singapore 119260

<sup>#</sup> Institute of Materials Research & Engineering, 3 Research Link, Singapore 117602

A critical issue in the fabrication of gallium nitride (GaN) devices is the achievement of significant and controllable *p*-type doping. Although magnesium (Mg) has been successfully and widely used as in-situ acceptor during GaN growth, there exists some disadvantages such as a large ionization energy (150-165 meV)<sup>1</sup>, limited solubility in GaN, high vapour pressure and low sticking coefficient.

Beryllium (Be) is considered a shallower acceptor in GaN due to its large electronegativity and the absence of *d*-electrons<sup>2</sup>. An *ab initio* calculation<sup>3</sup> predicted a thermal ionization energy of 60 meV for Be shallow acceptor in wurtzite GaN. Experimental evidences from photoluminescence (PL) showed its optical ionization energy ranging from 90-100 meV<sup>4,5</sup>, 150 meV<sup>6</sup>, to 250 meV<sup>7</sup>. Be atoms are likely to occupy interstitial sites (Be<sub>int</sub>) rather than substitutional sites (Be<sub>Ga</sub>) in GaN, due to its small size. A theoretical calculation<sup>8</sup> has pointed out that the formation energy of Be<sub>int</sub> is much less than that of Be<sub>Ga</sub>. Interstitial Be behaves like a double donor so that self-compensation is a drawback for the use of Be as an acceptor. That is why there is almost no achievement of electrical activation of Be-doped GaN, except for Brandt *et al.* who obtained high mobility *p*-type materials from Be-O codoped cubic GaN by molecular beam epitaxy.<sup>9</sup> Due to its toxicity and the unavailability of suitable Be precursors for metal organic chemical vapor deposition (MOCVD), Be was introduced into GaN layer either during growth by molecular beam epitaxy (MBE)<sup>4,5,7,9</sup>, or by ion implantation.<sup>6,10</sup>

In this paper, we investigate the electrical and structural properties of Be-implanted GaN under different annealing conditions. A new annealing process is proposed to achieve the *p*-type doping. Raman scattering and high resolution X-ray diffraction (XRD) were used to monitor the crystalline quality and structure.

Unintentionally doped ( $n \sim 10^{17} \text{ cm}^{-3}$ ) GaN layers, 2  $\mu\text{m}$  thick, were grown by MOCVD on *c*-plane sapphire substrate in a multiwafer rotating disk reactor at 1040 °C, with a  $\sim 20 \text{ nm}$  GaN buffer layer grown at 530 °C in advance. Be was implanted into two pieces of the undoped GaN wafer at 40 keV. The doses were  $3 \times 10^{14} \text{ cm}^{-2}$  and  $1 \times 10^{15} \text{ cm}^{-2}$ . Annealing was performed in a RTP system equipped with halogen-tungsten lamps. One set of the Be-implanted samples was sequentially annealed at 900 -1100 °C for 45 s in flowing N<sub>2</sub> according to a face-to-face geometry. The other set of Be-implanted samples was annealed in forming gas (12% H<sub>2</sub> and 88% N<sub>2</sub>) first at temperatures ranging from 500 to 1100 °C and then in flowing N<sub>2</sub> at 1100 °C.

From the variable temperature Hall measurements, a plot of the sheet carrier concentration/ temperature product ( $p_s T^{-3/2}$ ) vs. reciprocal temperature can be constructed. Figure 1 shows such a plot for a Be-implanted GaN sample annealed at 600 °C for 10 s in forming gas first, followed at 1100 °C for 45 s in N<sub>2</sub>. The activation energy of Be in GaN extracted from the plot is 127 meV, indicating the shallower acceptor level in GaN. Thermal probe measurements were performed to confirm the realization of *p*-type doping. We used Mg-doped *p*-type GaN and undoped *n*-type GaN samples as references. The results were consistent with the Hall measurements, thus confirming that the Be-implanted and annealed samples were indeed *p*-type. The sheet hole concentration of this sample at room temperature is around  $10^{13} \text{ cm}^{-2}$ . The new annealing process for the high dose ( $1 \times 10^{15} \text{ cm}^{-2}$ ) implanted samples produced high-resistivity material. More electrical data from room temperature Hall measurements were reported elsewhere,<sup>11</sup> in which we also pointed out that there appears to be some relationship between the enhanced diffusion of Be in the new annealing process and the activation of the acceptors, as indicated by secondary ion mass spectroscopy (SIMS) analysis.

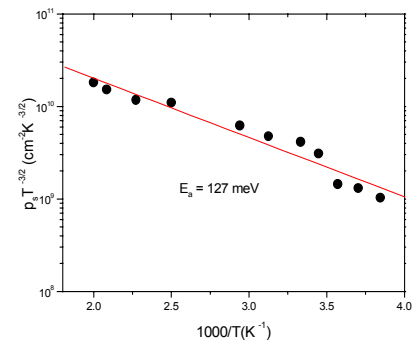


**FIG.1** Arrhenius plot of the sheet carrier concentration/ temperature product of Be-implanted GaN annealed in forming gas first, followed in N<sub>2</sub>, the dose is  $3 \times 10^{14} \text{ cm}^{-2}$

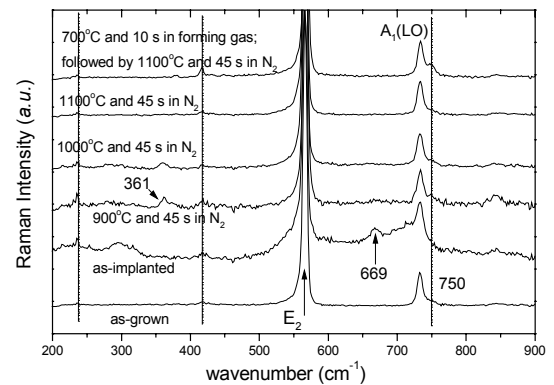


**Fig. 2.** Raman spectra of Be-implanted GaN at various conditions. The implantation dose is  $1 \times 10^{15} \text{ cm}^{-2}$

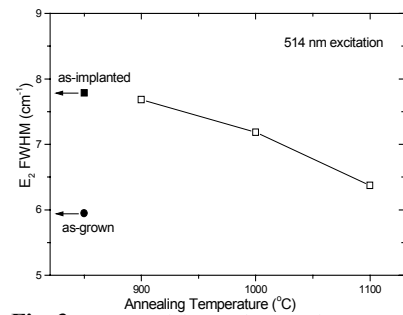
Figure 2 shows the Raman spectra of as-grown, Be-implanted and annealed GaN samples, excited with a 514 nm Ar<sup>+</sup> laser and measured at room temperature in backscattering Z(...)Z geometry with z direction along the c axis. For the as-grown sample, two lines due to the E<sub>2</sub> and A<sub>1</sub> longitudinal optical (LO) modes are observed as expected from the Raman selection rules in wurtzite semiconductor. The spectra shown are normalised to the E<sub>2</sub> phonon energy. The weak line at 418 cm<sup>-1</sup> stems from the sapphire substrate and the mode at 750 cm<sup>-1</sup> is a reminiscent of the E<sub>g</sub> sapphire mode. After implantation, three additional peaks appear at 300, 361 and 669 cm<sup>-1</sup>. The background signals also increase. The broad band at 300 cm<sup>-1</sup> was attributed to amorphous component.<sup>12</sup> We note that the mode at 361 cm<sup>-1</sup> exhibits a pronounced intensity when annealed at 900°C in N<sub>2</sub>, but not obvious in the as-implanted sample. The mode at 669 cm<sup>-1</sup> decreases simultaneously. Dislocations can grow at high temperature. So the peak at 361 cm<sup>-1</sup> and 669 cm<sup>-1</sup> may result from dislocations and less complex defects respectively.<sup>12</sup> Further increase of annealing temperature will minimize all modes introduced by implantation. The relation of the full width at half maximum (FWHM) of the E<sub>2</sub> mode versus temperature is plotted in figure 3. As shown, annealing at 1100 °C for 45 s almost restores the crystalline quality. The new annealing process has produced similar Raman signals as shown in Fig.2 and almost same value of E<sub>2</sub> FWHM. Our results also indicate that prior annealing in forming gas in prior affect the crystal quality significantly.

Figure 4 shows the HRXRD (0002) spectra for Be-implanted GaN samples. A new peak appears at the left side of the virgin (0002) peak of the implanted GaN and this can be attributed to the lattice expansion caused by the incorporation of Be into interstitial sites. After annealing in high temperature of 900 °C (not shown in Fig.4), there is only one diffraction peak observed. The FWHM after the new annealing process is 0.066°, even smaller than that of as-grown sample (0.069°). It indicates that the crystal structure has recovered and some micro-strains after growth relaxed. This is consistent with the observation of the Raman spectra. From the calculation of the lattice constant ratio d<sub>1</sub>/d<sub>0</sub> for Be implanted GaN, where d<sub>1</sub> and d<sub>0</sub> are the lattice constant for the implanted region and for the undoped region of GaN respectively. The lattice constant changes along c axis are ~0.39% and 0.53%, for 3×10<sup>14</sup> cm<sup>-2</sup> and 1×10<sup>15</sup> cm<sup>-2</sup> respectively. This indicates that higher dose implantation has introduced a larger strain along c axis.

In conclusion, p-type doping of GaN was achieved through a new annealing process for Be-implanted GaN. Structural properties were examined by means of Raman and HRXRD measurements. The post annealing process can almost restore the crystal structure of the implanted region, although some point defects still remains.

## Reference

- [1] I. Akasaki, H. Amano, M. Kito and K. Hiramatsu, *J. Lumin.*, **48/49**, 666 (1991)
- [2] S. Strite, *Jpn. J. Appl. Phys.*, **33**, 699 (1994)
- [3] F. Bernardini, V. Fiorentini, and A. Bosin, *Appl. Phys. Lett.*, **70**, 2990 (1997)
- [4] D. J. Dewsnap, A. V. Andrianov, I. Harrison, J. W. Orton, D.E. Lacklison, G. B. Ren, S.E. Hopper, T. S. Cheng, and C. T. Foxon, *Semicond. Sci. Tech.*, **13**, 500 (1998)
- [5] F. J. Sanchez, F. Calle, M. A. Sanchez-Garcia, E. Calleja, E. Munoz, C. H. Molly, D. J. Somerford, F. K. Koschnick, K. Michael, and J. M. Spaeth, *MRS Internet J. of Nitride Semicon. Research*, V3, Article 19 (1998)
- [6] C. Ronning, E. P. Carlson, D. B. Thomson, and R. F. Davis, *Appl. Phys. Lett.*, **73**, 1622 (1998)
- [7] A. Salvador, W. Kim, O. Aktas, A. Botchkarev, Z. Fan, and H. Morkoc, *Appl. Phys. Lett.*, **69**, 2692 (1996)
- [8] J. Neugebauer and C. G. Van De Walle, *Appl. Phys. Lett.*, **85**, 3003 (1999)
- [9] O. Brandt, H. Yang, H. Kostial, and K. H. Ploog, *Appl. Phys. Lett.*, **69**, 2707 (1996)
- [10] J. I. Pankove and J. A. Hutchby, *J. Appl. Phys.*, **47**, 5387 (1976)
- [11] Y. J. Sun, L. S. Tan, S. J. Chua, and S. Prakash, *MRS Internet J. of Nitride Semicon. Research*, accepted for publication
- [12] W. Limmer, W. Ritter, R. Sauer, B. Mensching, C. Liu, B. Rauschenbach, *Appl. Phys. Lett.*, **72**, 2589 (1998)



**Fig. 3.** FWHM of the E<sub>2</sub> phonon of as-grown and of Be-implanted as function of annealing temperature

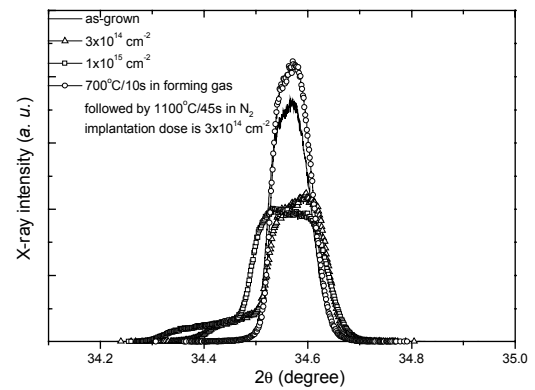


**Fig. 4.** (0002) XRD spectra for the as-grown, as-implanted and annealed samples